

# Enhancement of UAV-based Spatial Positioning Using the Triangular Center Method with Multiple GPS

Joo, Yongjin<sup>1)</sup> · Ahn, Yushin<sup>2)</sup>

## Abstract

Recently, a technique for acquiring spatial information data using UAV (Unmanned Aerial Vehicle) has been greatly developed. It is a very crucial issue of the GIS (Geographic Information System) mapping system that passes way point in the unmanned airframe and finally measures the accurate image and stable localization to the desired destination. Though positioning using DGPS (Differential Global Navigation System) or RTK-GPS (Real Time Kinematic-GPS) guarantee highly accurate, they are more expensive than the construction of a single positioning system using a single GPS. In the case of a low-priced single GPS system, the stability of the positioning data deteriorates. Therefore, it is necessary to supplement the uncertainty of the absolute position data of the UAV and to improve the accuracy of the current position data economically in the operating state of the UAV. The aim of this study was to present an algorithm enhancing the stability of position data in a single GPS mode of UAV with multiple GPS. First, the arrangement of multiple GPS receivers through the center of gravity of the UAV were examined. Next, MD (Mahalanobis Distance) is applied to detect instantaneous errors of GPS data in advance and eliminate outliers to increase the accuracy of previously collected multiple GPS data. Processing procedure for multiple GPS reception data by applying the center of the triangular method were presented to improve the position accuracy. Second, UAV navigation systems integrated multiple GPS through configuration of the UAV specifications were implemented. Using the unmanned airframe equipped with multiple GPS receivers, GPS data is measured with the TCM (Triangular Center Method). In addition, UAV equipped with multiple GPS were operated in study area and locational accuracy of multiple GPS of UAV with VRS (Virtual Reference Station) GNSS surveying were compared. The result showed that the error factors are compensated, and the error range are reduced, resulting in the reliability of the corrected value. In conclusion, the result in this paper is expected to realize high-precision position estimation at low cost in UAV using multiple low-cost GPS receivers.

Keywords : UAV, Multiple GPS, TCM, MD

## 1. Introduction

Recently, a technique for acquiring spatial information data using UAV (Unmanned Aerial Vehicle) has been greatly developed. In the existing position system such as total station and GPS (Global Positioning System), it is being gradually replaced with unmanned aerial vehicles due to the difficulty of direct measurement in the field with a lot of manpower and time for accurate positioning (Kim, 2018). A DEM (Digital Elevation Model) and a DSM (Digital Elevation

Model) based on an UAV have been developed to analyze the accurate status of road management and facilities (Joo, 2017; Feng *et al.*, 2014), as well as analysis and accuracy of 3D spatial information (Uysal *et al.*, 2015; Eker *et al.*, 2018; Lee and Sung, 2016). Positioning and utilization of spatial information by UAV are superior to conventional methods in terms of speed, economy and convenience. In addition, due to the characteristics of UAV, it is possible to collect current information and analyze and map spatial information for safety prevention and prompt response in disasters

Received 2019. 10. 03, Revised 2019. 10. 15, Accepted 2019. 10. 23

1) Member, Dept. of Aerial Geoinformatics, Inha Technical College (E-mail: [jjy@inhac.ac.kr](mailto:jjy@inhac.ac.kr))

2) Corresponding Author, Dept of Civil and Geomatics Engineering, California State University, Fresno, United States (E-mail: [yahn@csufresno.edu](mailto:yahn@csufresno.edu))

This is an Open Access article distributed under the terms of the Creative Commons Attribution Non-Commercial License (<http://creativecommons.org/licenses/by-nc/3.0>) which permits unrestricted non-commercial use, distribution, and reproduction in any medium, provided the original work is properly cited.

areas, where directly access is limited because of many obstacles (Kim *et al.*, 2014; Shin *et al.*, 2017; Um, 2018; Kwon *et al.*, 2019). Especially UAV are becoming increasingly used in environmental and natural disaster monitoring, precise surveying of cultural properties, border surveillance, emergency assistance, search and rescue missions and relay communications (Vacca and Onishi, 2017; Cole *et al.*, 2009; Van *et al.*, 2018; Hayat *et al.*, 2016; Erdelj *et al.*, 2017).

It is a very crucial issue of the GIS (Geographic Information System) mapping system that passes way point in the unmanned airframe and finally measures the accurate image and stable localization to the desired destination. The navigation system in UAV not only obtains the current location information of UAV through GPS, but also enables stable flight course and path planning through the setting of the way point (WP) that the unmanned airframe will fly. Positioning using DGPS (Differential Global Navigation System) or RTK-GPS (Real Time Kinematic-GPS) guarantee highly accurate but they are more expensive than the construction of a single positioning system using a single GPS. However, in the case of a low-priced single GPS system, the stability of the positioning data deteriorates. Therefore, it is necessary to supplement the uncertainty of the absolute position data of the UAV and to improve the accuracy of the current position data economically in the operating state of the UAV.

This study aimed to suggest an algorithm enhancing the stability of position data of UAV in a single GPS mode using multiple GPS. Newly designed framework for an unmanned positioning were developed by using a low-cost multiple GPS receiver installed in the UAV, which is enabled to reduce the distance errors by calibrating more accurately the position. In addition, multiple GPS receivers equipped with UAV are arranged according to the TCM (Triangular Center Method) and operated in the case study area to compare and analyze the position accuracy. To achieve our goal in this study, the research methods and procedures are as follows. First, in chapter 2, we mainly dealt with design of an algorithm for the TCM with multiple GPS. Then, the arrangement of multiple GPS receivers through the center of gravity of the UAV and the error range according to the number of GPS receivers were examined. Next, we designed processing procedure for multiple GPS reception data and propose a

method to improve the position accuracy of GPS by applying the pre-processing process and the center of the triangular method. In chapter 3, we configured the UAV specifications used in the empirical research and suggest implementing UAV navigation systems with multiple GPS to efficiently operate the equipment. Using the unmanned airframe equipped with multiple GPS receivers, GPS data is measured with the TCM. A precision VRS (Virtual Reference Station) receiver surveyed the location of benchmarks selected for the way point within flight capture area to verified coordinate accuracy and stability by comparing data of multiple GPS of UAV and VRS surveying position data. Fig. 1 shows the flow and content of the overall study.

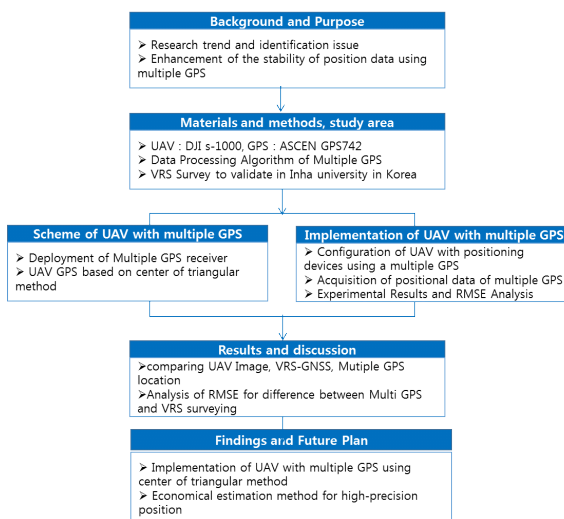


Fig. 1. Overview of study procedure

## 2. Scheme of UAV with Multiple GPS

### 2.1 Deployment Design of Multiple GPS Receiver

The GPS data contains various information such as time and the number of satellites receivable at the latitude and longitude, the traveling speed, and the moving direction. The slower speed the UAV moves, the more frequent phenomenon of the data jumps or the larger the error has. Especially, in the case of stationary positioning, there are many variables that are difficult to obtain stable data depending on time and environment. In addition, due to the characteristics of the hardware itself, there is a difference in data acquisition

performance between GPS modules. Fig. 2 shows the center of gravity and the error range of the UAV according to the number of GPS receivers (Choi *et al.*, 2013; Kim *et al.*, 2013; Moon *et al.*, 2008), Fig. 2(a) shows that the circle is assumed to be an error range of GPS, and the triangle in (b) and the rectangle in (c) represent the average error range of the whole receiver through the error range of each GPS receiver. When two GPS receivers are used, the position range is calculated through the average of the two received points, so the error range is wide as shown in Fig. 2 (a), In addition, the direction between two points is instantaneously changed at the moment of rotation, and the position error becomes larger. the position of the GPS receiver is approximated by using the TCM, so that the error range can be minimized as shown in Fig. 2 (b), In addition, it is possible to estimate the position more flexibly at the moment of instantaneous rotation. On the other hand, if more than four receivers are used, the center of gravity is obtained by using the center of gravity of the triangle as shown in Fig. 2 (c), the variation of the center of gravity becomes large and the error range becomes widened. Therefore, this increases the instantaneous error in rotation.

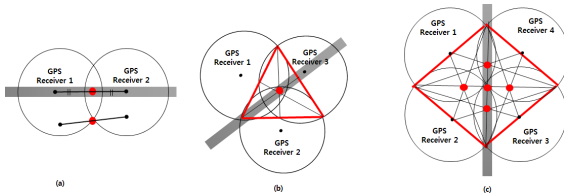


**Fig. 2. Weighted center and error range of UAV according to the number of GPS**

## 2.2 GPS Receiver based on TCM

In this paper, a system that minimizes the error range considering the number of receivers were designed. The GPS receiver can be arranged in a triangular shape as shown in Fig. 3. Then, the center point where the reception range of the GPS receiver overlaps can be determined as the position of the UAV airframe. When the position of the GPS receiver is approximated by the center of gravity, the error range can be minimized by using the TCM in which three GPS receivers are arranged in a triangular shape. The position can be measured more flexibly even during instantaneous rotation. Fig. 3 shows a method of applying the TCM to the arrangement

structure of the GPS receiver in the UAV airframe including the positioning device. Three GPS receivers with one receiver on the front and two receivers on the rear were designed and mounted on a real UAV airframe by applying a TCM. Fig. 3 (a) shows the unmanned airframe with three support fixture and a radial GPS fixed pedestal with the same angle and length of 120 degrees from each other at the center. Fig. 3 (b) shows the arrangement of the GPS receiver in the UAV airframe including the positioning device. The UAV includes three GPS receivers mounted on three support fixtures. GPS receivers are placed in equilateral triangles to receive various data from satellites without error and to reduce interference between GPS receivers. Therefore, the first GPS receiver, the second GPS receiver, and the third GPS receiver are arranged in a triangular shape among them.

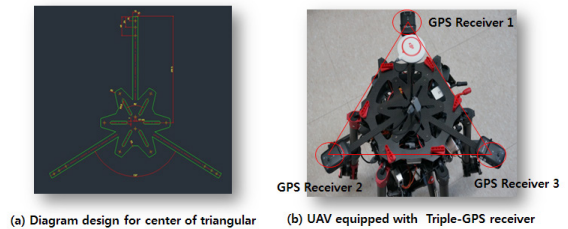


**Fig. 3. Arrangement of the GPS receives for the TCM**

## 2.3 Data Processing Algorithm of Multiple GPS

### 2.3.1 GPS Data Reception

When the GPS data transmission starts from the satellite, the GPS data includes information relating to the current position or speed of movement of the GPS receiver and metadata about the GPS data. 1st GPS receiver or 3rd GPS receiver included in the positioning device receives GPS data from at least one satellite. The processor of the positioning device analyzes the received data to the 1st or 3rd GPS receiver. The stability of the GPS receiver is determined by confirming that all data are received at the same time and the number of satellites connected to each GPS receiver is equal to or greater than a predetermined number 4.

### 2.3.2 Data Preprocessing

In order to increase the accuracy of previously collected multiple GPS data, MD (Mahalanobis Distance) is applied to detect instantaneous errors of GPS data in advance

and eliminate outliers. MD has a function in which the standard deviation and the correlation coefficient indicating the properties of a variable are considered together. As a result, more accurate absolute position information can be determined.

$$MD_i = \left( [x_i \ y_i] - [\hat{x}_t \ \hat{y}_t] \right)^T \left[ \sum_i \right]^{-1} \left( [x_i] - [\hat{x}_t] \right) \quad (1)$$

where,  $i$  is a gps,  $\sum_i$  is a covariance matrix

If it is determined that the stability is insufficient, the currently received data is excluded from the positioning process and additional GPS data is received from the satellites. And repeats the process of determining the stability of the GPS receiver from the received GPS data. If the reliability of the GPS is not ensured, the present position can be estimated by using the direction, speed and the direction angle of the moving UAV object at a point where the position is already known. If the position of the unmanned aircraft at time  $t$  is known, the position at time  $t + \Delta t$  is determined as follows.

$$\begin{aligned} x(t + \Delta t) &= x(t) + V \cos \theta \Delta t \\ y(t + \Delta t) &= y(t) + V \sin \theta \Delta t \end{aligned} \quad (2)$$

Also, assuming that the unmanned aerial vehicle makes a straight line motion when flying toward the way point, when the jump phenomenon of GPS data occurs, the position data obtained from the Eq. (2) is greatly deviated. To overcome this problem, the geometrical configuration of latitude and longitude is divided into four parts based on the direction of magnetic north at the present location, and linear regression analysis is performed on the characteristics of GPS data using velocity and azimuth, Respectively. Let  $Lon$  be the longitude,  $Lat$  be the latitude,  $t$  be the time, and  $a$  and  $b$  are the estimated coefficients, then the least squares method of regression analysis can be used as shown in Eq. (3),

$$\begin{aligned} Lon_n &= a_1 + b_1 x_1, Lat_n = a_2 + b_2 x_2 \\ a_1 &= \frac{\sum Lon_t}{n} = \frac{\sum y_{1i}}{n}, a_2 = \frac{\sum Lat_t}{n} = \frac{\sum y_{2i}}{n}, \\ b_1 &= \frac{\sum x_{1i} Lon_i}{\sum x_{1i}^2} = \frac{\sum x_{1i} y_{1i}}{\sum x_{1i}^2}, b_2 = \frac{\sum x_{2i} Lon_i}{\sum x_{2i}^2} = \frac{\sum x_{2i} y_{2i}}{\sum x_{2i}^2} \end{aligned} \quad (3)$$

### 2.3.3 Correction of Received Position Data

After determining whether the data of three receivers are reliable In the previous step, the position is corrected by the center of gravity of the triangle using the position data of the stable moment of each receiver in order to secure the reliability of the data continuously. Eq. (1) is a calculation formula of the position of each GPS receiver and multiple GPS receivers.  $G$  is a GPS receiver, and  $n$  is the number of satellites measured at the receiver. Here, the position value of the receiver having a large number of satellites is weighted. If the three receiver data are all good, the center of gravity is determined using the shape of a triangle. If two data are determined to be reliable, the average of the two data is calculated. When only one piece of GPS data is reliable, it takes an independent positioning format and receives data. If the number of satellites in the GPS receiver is less than four, the data is excluded.

$$\begin{aligned} P(G_1) &= \{x_{G1}, y_{G1}\} \\ P(G_2) &= \{x_{G2}, y_{G2}\} \\ P(G_3) &= \{x_{G3}, y_{G3}\} \\ P(CG) &= \sum_{i=1}^3 \left( \frac{G_i \times n_i}{n_i} \right) = \left\{ \frac{G_1 \times n_1 + G_1 \times n_2 + G_3 \times n_3}{n_1 + n_2 + n_3} \right\} \end{aligned} \quad (4)$$

The overall positioning procedure for UAV with multiple GPS receivers as shown in Fig. 4

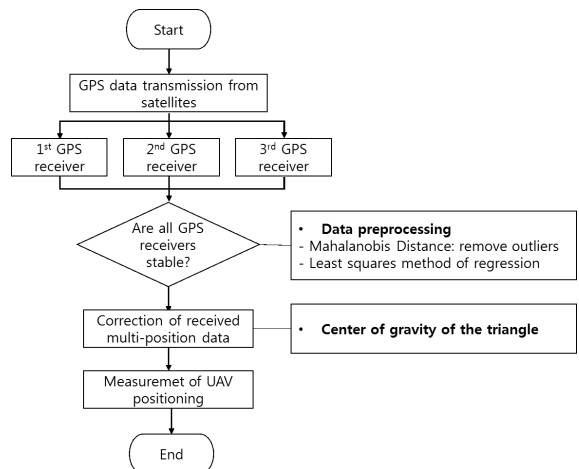


Fig. 4. Positioning procedures for multiple GPS receivers

### 3. Implementation of UAV with Multiple GPS





#### 3.1 Configuration of UAV with Positioning Devices Using a Multiple GPS

Table 1 shows the configuration of a UAV with positioning devices of a multiple GPS used in this study. The frame of the UAV used in this study is DJI S1000 model and includes 8 propellers and landing gear which can be folded in flight. One propeller output is up to 2.5kg and can be operated with a maximum weight of 20kg. The GPS receiver consists of ASCEN GPS742 with a single positioning error of less than 10 meters. The controller adopts DJI's A2 controller and iSOD II video transceiver, which are products of the same company, in consideration of convenience and compatibility between products. We used two units of the Futaba T14SG controller for UAV handling and camera operation. The camera was determined to be Panasonic's GH4 with 16 million pixels.

Fig. 5 shows the UAV equipped with multiple GPS by TCM implemented in this study. As shown in Fig. 5(a), we equipped the unmanned aerial vehicle with a radial GPS fixed pedestal that included support fixture with three identical length at 120 degrees from each other in the center. The GPS fixture includes a plurality of openings into which a screw or bolt can be inserted. It also includes a number of supports of the same length that are spread at a certain angle.

The radial GPS fixed mount is physically connected to the body of the unmanned aerial vehicle. Pedestal of the radial GPS is fixed to the upper end of the unmanned frame, and connects the body of the UAV as shown Fig. 5(b), Multiple GPS receivers were mounted on the three support fixture of the GPS installed in the unmanned airframe as shown Fig. 5(c), The three GPS receivers were installed on three support fixture extending from the center of the unmanned airframe as shown Fig. 5(d), Under the elongated support structure, the GPS can receive radio waves without interference from other equipment in the unmanned aerial vehicle. In order to ensure safety distance, the propeller included in the unmanned airframe was designed with a GPS device and a long extended GPS receiver as shown Fig. 5(e), The GPS receiver is located outside the turning radius of rotation of the propeller. A GPS receiver is positioned between the turning radius formed by the multiple propellers. Fig. 5 (f) is the final assembly of unmanned airframe with multiple GPS including the positioning device extends in three directions from the center by TCM.

**Table 1. Configuration of UAV**

	FLAME	GPS	Remote control	Controller
Model	 DJI S-1000	 ASCEN GPS742	 FUTABA T14SG (T/R Set)	 DJI A2+iOSD II Combo
Spec.	<ul style="list-style-type: none"> <li>• Frame Weight : 1330g</li> <li>• Diagonal Wheelbase : 1,045mm</li> </ul>	<ul style="list-style-type: none"> <li>• Weight: 64g</li> <li>• Chipset: MTK 66 channels</li> <li>• Working distance: Within 10m</li> <li>• GPS connection time: less than 36s</li> <li>Channel: 66</li> </ul>	<ul style="list-style-type: none"> <li>• Basic 5-channel 2.4GHz</li> <li>• DSMXradio and receiver</li> </ul>	<ul style="list-style-type: none"> <li>• RTH (Return-To-Home)</li> <li>• IOC(Intelligent Orientation Control)</li> <li>• Low Battery Warning</li> </ul>



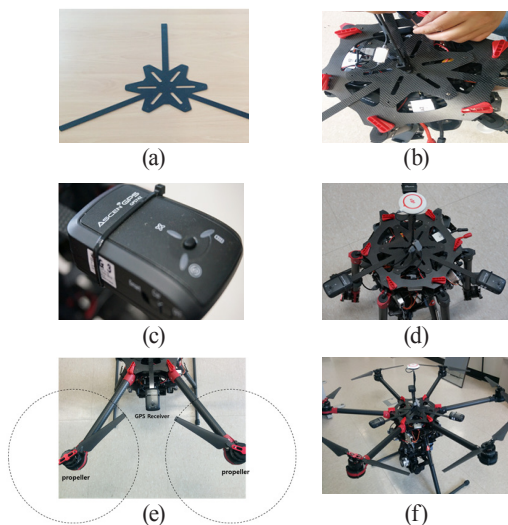


Fig. 5 UAV assembly of multiple GPS by TCM

### 3.2 Acquisition of Positional Data of Multiple GPS

In order to improve the accuracy of UAV's outdoor single location estimation, we used the position of the TCM using multiple GPS above mentioned in 3.1 compensating the positional information of single GPS with relatively large error. For the experiment, coordinates were obtained for the roads inside Inha University. The coordinates of GPS and the location of GCP are as shown in Fig. 6.

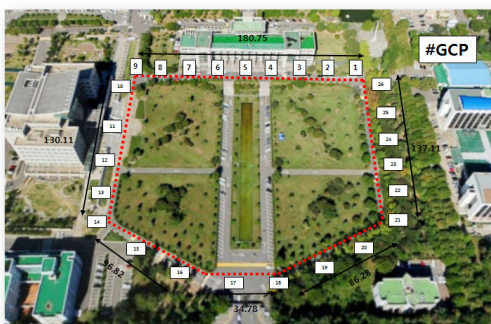


Fig. 6. Study area

Fig. 7 shows that multiple GPS data of the unmanned aerial vehicle captured by the flight and the position data of the VRS GNSS surveying to be converted and displayed on the GIS map. Fig. 7(a), (b) and (c) show reception logs of three individual GPS, and Fig. 7(e) Three GPS receivers were used

to obtain the positional information corrected by the TCM. A total of 26 GCP locations as a benchmark for way points in the unmanned aerial photographing area were obtained by using VRS surveying receiver (Kolida K9-T) as shown in Fig. 7(f),

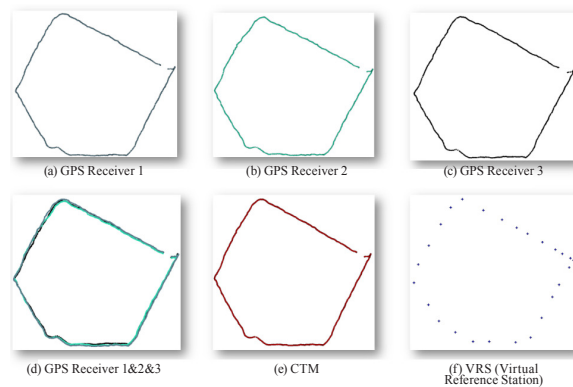


Fig. 7. GIS map for the position data of multiple GPS and the VRS survey

Table 2 shows the results of survey by individual GPS receiver and VRS survey.

### 3.3 Experimental Results and Analysis

The multiple GPS data of the unmanned aerial vehicle and the VRS survey location data were compared with each other to verify coordinate accuracy and stability. The experiment started from the initial ID (latitude: 37.44890102, longitude: 126.6549006) and moved to final ID21 (latitude: 37.44876104, longitude: 126.6551912), Table 3 shows the difference between VRS positions and the independent GPS and TCM. Positions of multiple GPS for the images acquired from the UAV and the passing way points, and the actual VRS GNSS was surveyed for the corresponding GCP as shown in Table 4. As a result of measuring the GCP position accuracy of the final 21 points, the RMSE was 1.651825m.

**Table 2. The result of individual GPS receiver and VRS survey (Unit: m)**



ID		Photo_id	GPS <sub>1</sub> _Long	GPS <sub>2</sub> _Long	GPS <sub>3</sub> _Long	TCM_Long	VRS_Long
1	R3	24	126.654896	126.654892	126.654872	126.6548867	126.6549006
2	R4	37	126.654687	126.654692	126.65468	126.6546863	126.6546883
3	R5	55	126.654436	126.654444	126.654424	126.6544347	126.6544485
4	R6	69	126.654276	126.654278	126.654265	126.654273	126.6542731
5	R7	89	126.654029	126.654026	126.65402	126.654025	126.654035
6	R8	108	126.653731	126.653738	126.65373	126.653733	126.6537339
7	R9	137	126.653383	126.653399	126.653373	126.653385	126.6533915
8	R10	152	126.653174	126.65322	126.653186	126.6531933	126.6532041
9	R11	172	126.653	126.653023	126.653013	126.653012	126.6530442
10	R12	197	126.652816	126.65283	126.652832	126.652826	126.6528531
11	R13	218	126.652672	126.652686	126.652681	126.6526797	126.6526835
12	R14	241	126.652618	126.652618	126.652628	126.6526213	126.6526162
13	R15	267	126.652827	126.652819	126.652836	126.6528273	126.6528481
14	R16	287	126.652987	126.652991	126.652998	126.652992	126.6530211
15	R18	327	126.653564	126.653562	126.653577	126.6535677	126.6535749
16	R19	342	126.653827	126.653818	126.653839	126.653828	126.6538363
17	R20	374	126.654255	126.654244	126.654261	126.6542533	126.6542619
18	R22	411	126.654679	126.654652	126.654663	126.6546647	126.6546794
19	R23	438	126.654854	126.654823	126.654845	126.6548407	126.6548546
20	R25	474	126.655105	126.655083	126.655103	126.655097	126.655124
21	R26	483	126.655163	126.655153	126.655163	126.6551597	126.6551912
ID		Photo_id	GPS <sub>1</sub> _Lat	GPS <sub>2</sub> _Lat	GPS <sub>3</sub> _Lat	TCM_Lat	VRS_Lat
1	R3	24	37.448911	37.448895	37.448906	37.448904	37.44890102
2	R4	37	37.449007	37.44899	37.449001	37.44899933	37.44899661
3	R5	55	37.449117	37.449094	37.449106	37.44910567	37.44910589
4	R6	69	37.449199	37.449176	37.449191	37.44918867	37.44918364
5	R7	89	37.449294	37.449266	37.449288	37.44928267	37.44928602
6	R8	108	37.449414	37.449396	37.449417	37.449409	37.44940975
7	R9	137	37.44956	37.44954	37.44954	37.44954667	37.4495516
8	R10	152	37.449466	37.449453	37.449442	37.44945367	37.44944437
9	R11	172	37.449224	37.449243	37.449212	37.44922633	37.4492236
10	R12	197	37.448956	37.448981	37.448947	37.44896133	37.4489473
11	R13	218	37.448685	37.448713	37.448683	37.44869367	37.44869965
12	R14	241	37.448458	37.448469	37.448456	37.448461	37.44846066
13	R15	267	37.448166	37.448172	37.448177	37.44817167	37.44817415
14	R16	287	37.447951	37.447954	37.447961	37.44795533	37.44796344
15	R18	327	37.447683	37.4477	37.447699	37.447694	37.44769938
16	R19	342	37.447674	37.447687	37.447698	37.44768633	37.44769801
17	R20	374	37.44769	37.447698	37.44771	37.44769933	37.44768985
18	R22	411	37.448009	37.448005	37.448017	37.44801033	37.44801081
19	R23	438	37.448289	37.448283	37.448287	37.44828633	37.44828183
20	R25	474	37.448665	37.44866	37.448669	37.44866467	37.44866745
21	R26	483	37.448767	37.448765	37.448772	37.448768	37.44876104

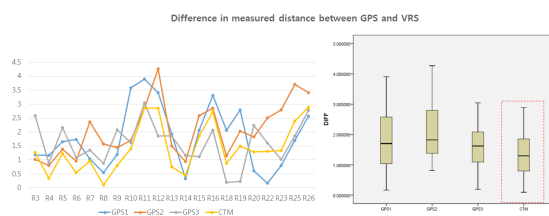
**Table 3. Difference distance between VRS and multiple GPS  
(Unit : m)**

ID		GPS1 Dxy	GPS2 Dxy	GPS3 Dxy	TCM Dxy
1	R3	1.186076	1.013917	2.584992	1.27405
2	R4	1.159159	0.80578	0.880642	0.342391
3	R5	1.65572	1.382668	2.165468	1.2235
4	R6	1.730291	0.954357	1.091031	0.553719
5	R7	1.035914	2.364536	1.346319	0.95907
6	R8	0.553719	1.571902	0.875507	0.094962
7	R9	1.193654	1.45264	2.08268	0.794509
8	R10	3.585996	1.704033	1.619931	1.40531
9	R11	3.902697	2.858342	3.041752	2.858342
10	R12	3.415995	4.266957	1.86329	2.856764
11	R13	1.918139	1.501482	1.865708	0.747732
12	R14	0.328958	0.940076	1.163043	0.455422
13	R15	2.071827	2.579754	1.115551	1.853585
14	R16	3.312801	2.858342	2.058728	2.722613
15	R18	2.060917	1.143494	0.189924	0.875507
16	R19	2.794531	2.027834	0.232609	1.495464
17	R20	0.608054	1.821688	2.243196	1.29511
18	R22	0.164479	2.501669	1.600329	1.302054
19	R23	0.800164	2.794531	1.022773	1.329469
20	R25	1.698733	3.714461	1.860868	2.404247
21	R26	2.576256	3.40277	2.773477	2.889719
RMSE		<b>2.101257</b>	<b>2.28971</b>	<b>1.77016</b>	<b>1.651825</b>

The jumping phenomenon of GPS data occurs, and the kinetic characteristics of the UAV are changed, giving rise to a somewhat unstable positioning result. Therefore, single GPS has a wide range of positional errors and a relatively large deviation. However, by using the TCM described above, the center of gravity of the unmanned airframe were captured and the stable motion characteristic can be seen from the initial start to the final destination. As shown in Fig. 8, the error factors are compensated and the error range and the instantaneous error are reduced, resulting in the reliability of the corrected value with a gentler shape.

**Table 4. UAV Image and VRS-GNSS (Unit : m)**

ID	UAV Image [TCM]	VRS-GNSS	Dxy
R9			0.794509
R12			2.856764
R14			0.455422
R18			0.875507

**Fig. 8. Comparison of distance difference between multiple GPS and VRS**

## 4. Conclusions

In our paper, newly-designed framework for an unmanned positioning were suggested by using a low-cost multiple GPS receiver installed in the UAV, which is enable to reduce the distance errors by calibrating more accurately the position. This study aimed to suggest an algorithm enhancing the stability of position data in a single GPS mode using multiple GPS. In addition, multiple GPS receivers equipped with UAV are arranged according to the TCM and operated in the case study area to compare and analyze the position accuracy. Single GPS has a wide range of positional errors and a relatively large deviation. However, the center of gravity of



the unmanned airframe by using the TCM were captured and the stable motion characteristic can be seen from the initial start to the final destination. The error factors are compensated, and the error range and the instantaneous error are reduced, resulting in the reliability of the corrected value with a gentler shape. In conclusion, the result in this paper is expected to realize high-precision position estimation at low cost in unmanned aerial vehicles using multi low-cost GPS receivers. Hereafter, it is expected that the accuracy may be improved if the comparison includes not only the planar position (X, Y) of the UAV but also the height value (Z) through the stereoscopic image acquisition.

## References

- Choi, S.H., Kim, Y.K., Hwang, Y.S., Kim, H.W., and Lee, J.M. (2013), EKF based outdoor positioning system using Multiple GPS receivers. *Journal of Korea Robotics Society*, Vol. 8, No. 2, pp.129-135. (in Korean with English abstract)
- Cole, D., Goktogan, A., Thompson, P., and Sukkarieh, S. (2009), Mapping and tracking. *IEEE Robotics Automation Magazine*, Vol. 16, No. 2, pp. 22–34.
- Eker, R., Aydın, A., and Hubl, J. (2018), Unmanned aerial vehicle (UAV)-based monitoring of a landslide: Gallenzerkogel landslide (Ybbs-Lower Austria) case study. *Environmental Monitoring and Assessment*, Vol. 190, No. 1, pp.1-28.
- Erdelj, M., Natalizio, E., Chowdhury, K. R., and Akyildiz, I. F. (2017), Help from the sky: Lever- aging UAVs for disaster management. *IEEE Pervasive Computing*, Vol. 16, No. 1, pp.24–32.
- Feng, H., Jiang, Z., Xie, F., Yang, P., Shi, J., and Chen, L. (2014), Automatic fastener classification and defect detection in vision-based railway inspection systems. *IEEE Transactions on Instrumentation and Measurement*, Vol. 63, No. 4, pp. 877-888.
- Hayat, S., Yanmaz, E., and Muzaffar, R. (2016), Survey on unmanned aerial vehicle networks for civil applications: A communications viewpoint. *IEEE Communications Surveys Tutorials*, Vol. 18, No. 4, pp. 2624–2661.
- Joo, Y. J. (2017), Detection method for road pavement defect of UAV imagery based on computer vision. *Journal of the Korean Society of Surveying, Geodesy, Photogrammetry and Cartography*, Vol. 35, No. 6, pp. 599-608. (in Korean with English abstract)
- Kim, D., Song, Y., Kim, Gi., and Kim, C. (2014), A study on the application of UAV for Korean land monitoring. *Journal of the Korean Society of Surveying, Geodesy, Photogrammetry, and Cartography*, Vol. 32, No. 1, pp. 29-38. (in Korean with English abstract)
- Kim, J. H. and Kim, J. H. (2018), Accuracy analysis of cadastral control point and parcel boundary point by flight altitude using UAV. *Journal of the Korean Society of Surveying, Geodesy, Photogrammetry and Cartography*, Vol. 36, No. 4, pp. 223-233. (in Korean with English abstract)
- Kim, Y.K., Choi, S.H., and Lee, J.M. (2013), Enhanced outdoor localization of Multi-GPS/INS fusion system using mahalanobis distance. *2013 10th International Conference on Ubiquitous Robots and Ambient Intelligence (URAI)*, 30 May, Jeju, Korea, pp. 488-492. (in Korean with English abstract)
- Kwon, J.Y., Kim, Y.W., and Choi, S.H. (2019), Airspace map design to implement customer-friendly service on unmanned aerial vehicles. *Spatial Information Research*, Vol. 27, No. 1, pp.87–95.
- Lee, J., and Sung, S. (2016), Evaluating spatial resolution for quality assurance of UAV images. *Spatial Information Research*, Vol. 24, No. 2, pp. 141 -154.
- Moon, H.C., Son, Y.J., and Kim, J. H. (2008), The development of driving algorithm for an unmanned vehicle with Multiple-GPS , *Journal of Institute of Control, Robotics and Systems*, Vol. 14, No. 1, pp. 27–35. (in Korean with English abstract)
- Shin, H., Um, J., and Kim, J. (2017), A study on damage scale tacking technique for debris flow occurrence section using drones image. *Journal of the Korean Society of Surveying, Geodesy, Photogrammetry, and Cartography*, Vol. 35, No. 6, pp. 517-526. (in Korean with English abstract)
- Uysal, M., Toprak, A.S., and Polat, N. (2015), DEM generation with UAV photogrammetry and accuracy analysis in Sahitler Hill. *Measurement*, Vol. 73, pp. 539-543.
- Um, J.S. (2018), Evaluating patent tendency for UAV related to spatial information in South Korea. *Spatial Information*

*Research*, Vol. 26, No. 2, pp. 143-150.

Vacca, A. and Onishi, H. (2017), Drones: military weapons, surveillance or mapping tools for environmental monitoring? The need for legal framework is required.

*Transportation Research Procedia*, Vol. 25, pp. 51–62.

Van Iersel, W., Straatsma, M., Addink, E. and Middelkoop, H. (2018), Monitoring height and greenness of non-woody floodplain vegetation with UAV time series. *ISPRS Journal of Photogrammetry and Remote Sensing*, Vol. 141, pp. 112–123.